

# UC San Diego

## UC San Diego Previously Published Works

### Title

Osimertinib regressed an EGFR-mutant lung-adenocarcinoma bone-metastasis mouse model and increased long-term survival

### Permalink

<https://escholarship.org/uc/item/13v2h4fh>

### Journal

Translational Oncology, 13(10)

### ISSN

1944-7124

### Authors

Higuchi, Takashi  
Sugisawa, Norihiko  
Park, Jun Ho  
et al.

### Publication Date

2020-10-01

### DOI

10.1016/j.tranon.2020.100826

Peer reviewed



## Original research

## Osimertinib regressed an EGFR-mutant lung-adenocarcinoma bone-metastasis mouse model and increased long-term survival



Takashi Higuchi <sup>a,b,c</sup>, Norihiko Sugisawa <sup>a,b</sup>, Jun Ho Park <sup>a</sup>, Yu Sun <sup>a,b</sup>, Guangwei Zhu <sup>a,b</sup>, Norio Yamamoto <sup>c</sup>, Katsuhiro Hayashi <sup>c</sup>, Hiroaki Kimura <sup>c</sup>, Shinji Miwa <sup>c</sup>, Kentaro Igarashi <sup>c</sup>, Michael Bouvet <sup>b</sup>, Shree Ram Singh <sup>d,\*</sup>, Hiroyuki Tsuchiya <sup>c,\*</sup>, Robert M. Hoffman <sup>a,b,\*\*</sup>

<sup>a</sup> *AntiCancer, Inc., San Diego, CA, USA*

<sup>b</sup> *Department of Surgery, University of California, San Diego, CA, USA*

<sup>c</sup> *Department of Orthopedic Surgery, Kanazawa University, Kanazawa, Japan*

<sup>d</sup> *Basic Research Laboratory, National Cancer Institute, Frederick, MD, USA*

## ARTICLE INFO

## Article history:

Received 1 May 2020

Accepted 15 May 2020

Available online xxx

## Keywords:

Osimertinib

Non-small-cell lung carcinoma

Bone metastasis

Orthotopic mouse model

## ABSTRACT

Bone is one of the most frequent metastatic sites in non-small cell lung cancer (NSCLC). Osimertinib, with and without bevacizumab (BV), has been investigated on advanced NSCLC patients. However, the efficacy of those drugs on bone metastasis of NSCLC has not been investigated. The human NSCLC cell line H1975, expressing red fluorescent protein (H1975-RFP), was orthotopically injected to the tibia of nude mice. The established mouse models were randomized into four treatment groups of nine mice: Control; BV alone; osimertinib alone; osimertinib and BV combination. The tumors were observed by non-invasive fluorescence imaging. Osimertinib, with or without BV, caused tumor regression, increased mouse survival, and bone remodeling in the bone metastasis models. These results suggest that osimertinib is a promising clinical option for NSCLC patients with bone metastasis.

© 2020 The Authors. Published by Elsevier Inc. on behalf of Neoplasia Press, Inc. This is an open access article under the CC BY-NC-ND license (<http://creativecommons.org/licenses/by-nc-nd/4.0/>).

## Introduction

Bone is one of the most frequent metastatic sites in non-small cell lung cancer (NSCLC) [1]. Approximately 30 to 40% of NSCLC patients develop bone metastasis during the course of disease [2]. The current treatment options for NSCLC with bone metastases include surgery, radiotherapy, and chemotherapy [3]. In addition to these treatments, bone-modifying agents such as zoledronic acid and denosumab (anti-receptor activator of nuclear factor-kappa B ligand antibody) are frequently used to prevent skeletal-related events (SREs) [4]. However, prognosis is still poor and median survival time is less than one year after the occurrence of bone metastases in NSCLC patients [2].

Metastatic NSCLC frequently involves epidermal growth-factor receptor (EGFR) gene mutation which determines the efficacy of EGFR tyrosine-kinase inhibitors (EGFR-TKIs) [5]. Pre-clinical studies have shown that EGFR-TKI and vascular endothelial growth-factor (VEGF) inhibitors work synergistically on tumors with EGFR mutations [6]. Erlotinib, a first-generation reversible EGFR-TKI, has been used for advanced EGFR mutation-positive NSCLC patients in combination with bevacizumab

(BV), a monoclonal antibody against VEGF [7]. Recently osimertinib, a third-generation irreversible EGFR-TKI, has been used for advanced EGFR mutation-positive NSCLC patients as monotherapy [8]. However the efficacy of the osimertinib and BV combination for NSCLC patients is still poorly understood [9]. In addition, osimertinib, either with or without BV, for bone-metastatic EGFR-mutated NSCLC has not been studied.

In the present study, we established an imageable orthotopic xenograft mouse model of H1975, an EGFR-mutated and T790M-positive NSCLC cell line, expressing red fluorescent protein (H1975-RFP) growing in the mouse tibia and determined the efficacy of osimertinib and osimertinib combined with BV.

## Materials and methods

## Cell line and cell culture

The H1975-RFP human EGFR-mutant NSCLC cell line with stable high-expression RFP (AntiCancer, Inc., San Diego, CA) was maintained in RPMI-1640 (Mediatech, Inc. Manassas, VA) with 10% fetal bovine serum. All

\* Corresponding authors.

\*\* Correspondence to: R.M. Hoffman, AntiCancer, Inc., San Diego, CA, USA.

E-mail addresses: [singhshr@mail.nih.gov](mailto:singhshr@mail.nih.gov), (S.R. Singh), [tsuchi@med.kanazawa-u.ac.jp](mailto:tsuchi@med.kanazawa-u.ac.jp), (H. Tsuchiya), [all@anticancer.com](mailto:all@anticancer.com). (R.M. Hoffman).

media were supplemented with penicillin and streptomycin. Cells were cultured at 37 °C with 95% air and 5% CO<sub>2</sub>.

## Mice

Athymic nu/nu nude mice (AntiCancer, Inc.) were used. The mouse investigations in the present report were carried out using an AntiCancer, Inc. Institutional Animal Care and Use Committee (IACUC) protocol specifically approved for this study as previously described and as per as the principles and procedures provided in the National Institutes of Health Guide for the Care and Use of Animals under Assurance Number A3873-1 [10,11]. To minimize any suffering of the animals, anesthesia and analgesics were used for all surgical experiments [10,11]. The mice were observed on a daily basis and humanely sacrificed by over-dosed anesthesia if they met the following humane endpoint criteria: severe tumor burden (more than 20 mm in diameter), prostration, significant body weight loss, difficulty breathing, rotational motion and body temperature drop [10,11].

## Establishment of bone injection NSCLC model

H1975-RFP cells growing in culture were washed with phosphate-buffered saline (PBS, Mediatech, Inc., Manassas, VA) and harvested by trypsinization. H1975-RFP cells ( $1 \times 10^6$ /PBS 10  $\mu$ L + Matrigel 10  $\mu$ L) were injected into the right tibia of nude mice using a 1 mL tuberculin syringe with a 27G1/2 needle (Fig. 1).

## Treatment study design

When average tumor area reached 50–100 mm<sup>2</sup>, the mouse models were randomized into 4 groups of 9 mice each: G1, control (corn oil + 10% DMSO, oral gavage, 28 consecutive days); G2, BV (bevacizumab 5 mg/kg, intraperitoneal injection [i.p.], twice per week); G3, osimertinib (25 mg/kg/day, oral gavage, 28 consecutive days); G4, osimertinib (25 mg/kg/day, oral gavage, 28 consecutive days) + BV (5 mg/kg, i.p., twice per week). Tumor size and mouse body weight were measured twice a week. Fluorescence imaging was with the FluorVivo (INDEC BioSystems, CA, Fig. 1). Data are presented as mean  $\pm$  standard error of the mean (SEM).

## Mice survival

Administration of all drugs ended 28 days after treatment initiation. The measurements of tumor size and body weight were continued to observe disease-free survival and overall survival after treatment ended. Each of the mice were sacrificed when net weight loss of more than 20%, tumor size reaching over 20 mm, or morbidity was observed in the mice. All observation of mouse survival ended 50 days after treatment ended (78 days after treatment initiation).

## Histological analysis

Fresh tumor samples were fixed in 10% formalin and embedded in paraffin before sectioning and staining. Tissue sections were deparaffinized in xylene and rehydrated in an ethanol series. Hematoxylin and eosin (HE) staining was performed according to standard protocol.

## Statistical analysis

All statistical analyses were performed with statistical software EZR (Saitama Medical Center, Jichi Medical University). Fisher's exact test was used for two categorical variables. A normal distribution was assessed with the Shapiro-Wilk test. The Bartlett's test was used to verify the homogeneity of variances among groups. One-way ANOVA with Tukey HSD for post hoc analysis was used for the parametric test for inter-group comparison. The paired *t*-test was used for the parametric test to compare the means between two related groups. Kruskal-Wallis with Steel-Dwass for post hoc analysis was used as the non-parametric test for inter-group comparison. All *p*-values were two sided and *p*-values of 0.05 or less were considered statistically significant.

## Results

### Efficacy of BV, osimertinib, and osimertinib + BV on H1975-RFP NSCLC growing in the bone

Osimertinib and osimertinib + BV regressed the NSCLC bone metastasis (Figs. 2, 3). There was no significant difference in the number of the

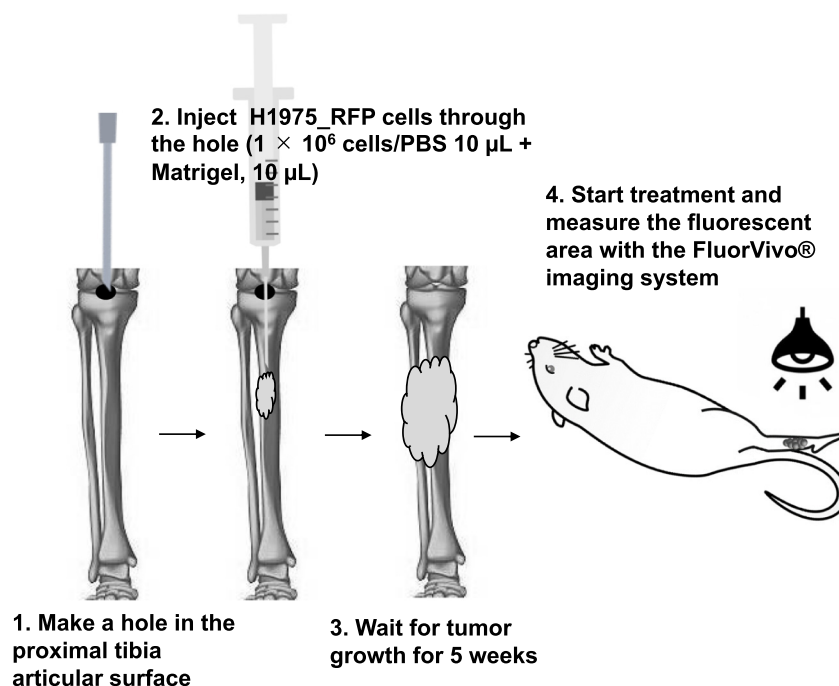


Fig. 1. Schema of establishment and observation of the non-small-cell lung cancer (NSCLC) bone-metastasis mouse model.

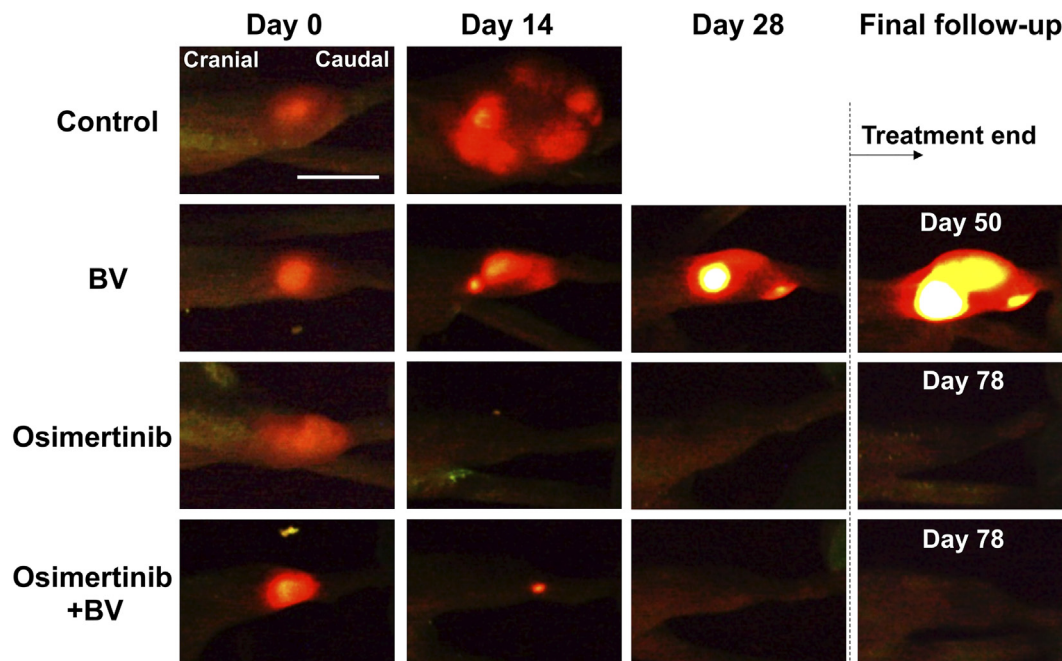


Fig. 2. Fluorescence images of representative red fluorescent protein (RFP)-expressing NSCLC growing in the tibia of nude mice, from each treatment group, at each time point after the onset of treatment.

mice with tumor regression between the osimertinib and osimertinib + BV groups ( $p = 1.00$ , Table 1) There were significant differences in tumor size at the final treatment day between osimertinib with/without BV and BV alone ( $p < 0.001$ , Fig. 3) BV alone inhibited tumor growth compared to the control group. The tumors grew rapidly and all of the mice were sacrificed by day 22 in the control group.

Overall and disease-free survival

All mice except mice in the control group survived the entire treatment period (Fig. 4A). Median survival time of mice in each group was 17 days in the control group; 50 days in BV-treated group, 78 days in the osimertinib-treated group, and 78 days in osimertinib + BV-treated group (Fig. 4A). There was no significant difference in overall survival between the osimertinib-treated and osimertinib + BV treated groups ( $p = 0.32$ , Table 2). RFP fluorescence was not detectable in 7 mice in the

osimertinib-treated group and 6 mice in the osimertinib + BV-treated group (Table 1). Median disease-free survival time after treatment ended was 28 days in each group and there was no significant difference between the groups ( $p = 0.93$ , Table 2 and Fig. 4B).

Histology of H1975-RFP growing in the bone

Fig. 5 shows the tumor histology of each group. The control tumor mainly comprised viable highly-dense cancer cells with nuclear atypia and mitosis which could be detected in high-power fields (HPF, Fig. 5A'). Invading cancer cells in the tumor section could be observed in low-power fields (LPF, Fig. 5A). Tumors treated with BV alone, which were fluorescently detectable at the sacrifice on the final observation day, also comprised highly-dense cancer cells detected, in both HPF (Fig. 5B') and LPF (Fig. 5B). However, the cancer-cell density was lower than that of control detected by LPF (Fig. 5B) and necrotic cells characterized by swelling and condensed nuclei were detected in HPF (Fig. 5B'). There were no residual cancer cells detected in mice with osimertinib alone and osimertinib + BV in either LPF or HPF. Bone remodeling after complete response to the treatment was observed (Fig. 5C, C' and D, D').

Effect of treatment on body weight

There was a significant difference in mouse body weight between the BV-treated group and osimertinib treated group ( $p < 0.001$ ) or osimertinib + BV-treated group ( $p = 0.01$ ) at the final treatment day (day 28, Fig. 6A). However, body weight increase in the BV treated group could be due to increased tumor-weight. There was a significant difference in body weight between pre- and post-treatment in the BV-treated group ( $p < 0.01$ ).

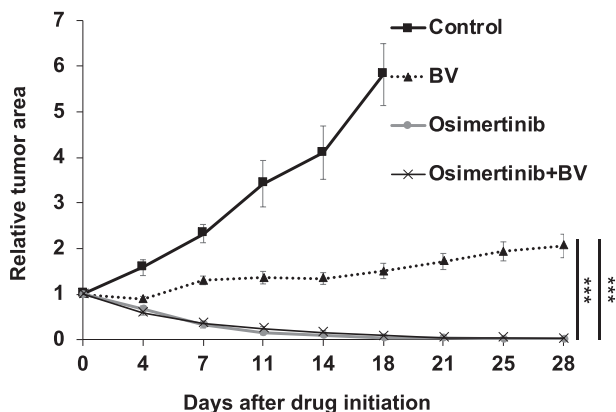


Fig. 3. Quantitative efficacy of drugs on the tumor size of RFP-expressing NSCLC growing in the tibia. Line graphs indicate tumor size at each time point after the onset of treatment relative to the initial tumor size for each treatment and control group. N = 9 mice/group. \*\*\*  $p < 0.001$ . Error bars:  $\pm$  SEM.

Table 1

Tumor regression at the final treatment day.

Tumor regression	Yes	No	p value
Osimertinib	7	2	1.00
Osimertinib + BV	6	3	



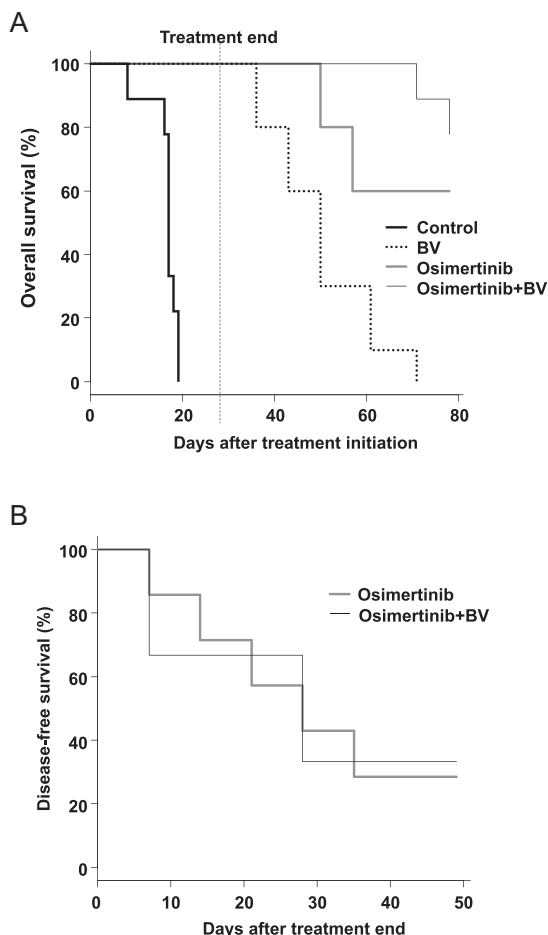


Fig. 4. (A) Overall survival curve after treatment initiation of each group. (B) Disease-free survival curve after treatment end of each group.

Table 2

Overall- and disease-free-survival after the treatment ended.

	n	p value
Overall survival		
Osimertinib	9	0.324
Osimertinib + BV	9	
Disease-free survival		
Osimertinib	7	0.925
Osimertinib + BV	6	

There was no significant difference between the osimertinib with or without BV-treated groups (Fig. 6B). There were no other observable side effects in any group.

Discussion

NSCLC is the third-most common cause of bone metastases, following breast and prostate cancer [2]. Bone-modifying agents are frequently used as palliative treatment for preventing pathological fracture. However, the use of chemotherapy drugs on bone metastatic NSCLC is still controversial [12]. In the present study, the efficacy of osimertinib alone and osimertinib combined with BV for NSCLC bone metastasis was evaluated in model of RFP-labeled EGFR-mutant NSCLC growing in the bone of nude mice.

Osimertinib is now used for the treatment of advanced EGFR-mutant NSCLC patients who have a good performance status [8,13]. We previously demonstrated the efficacy of osimertinib for brain metastasis of NSCLC using a GFP-labeled NSCLC brain-implant nude-mouse model [14]. However, the efficacy of osimertinib on bone metastasis of NSCLC has not been previously investigated. In the present study, we determined that osimertinib could regress EGFR-mutant NSCLC tumors growing in the bone and remodel the bone.

VEGF is overexpressed and circulating levels of VEGF are elevated in lung cancer [15], BV has been used for lung cancer treatment in combination with chemotherapy [7]. VEGF inhibition enhances the efficacy of EGFR-TKI in EGFR-mutated NSCLC cancer cells [16]. BV plus first-generation EGFR-TKI, erlotinib have been used for EGFR-positive advanced NSCLC patients with limited efficacy [7,17]. Clinical trials for the combination of BV and third-generation EGFR-TKI, osimertinib on EGFR-mutant lung cancers are now undergoing [18]. However, the efficacy of this combination for bone metastasis of NSCLC has not been investigated. In the present study, we were not able to demonstrate the advantage of the osimertinib plus BV combination, compared to osimertinib alone, because osimertinib alone regressed the bone metastasis. However, the overall survival of osimertinib +BV treated group tended to be longer than osimertinib alone, but there was not a significant difference. Growth inhibition of this rapid-growing bone tumor model by BV alone compared to control may also suggest the usefulness of adding BV to osimertinib for EGFR-mutated NSCLC bone- metastasis treatment. Future studies will include orthotopic implantation of both NSCLC cell lines and patient tumors in the lung that spontaneously metastasize to the bone [19].

In the present study, we implanted RFP-labeled EGFR-mutant NSCLC tumors orthotopically to the mouse bone to track the intraosseous tumors in real time and evaluate drug efficacy. The tumor regression and bone remodeling caused by osimertinib with or without BV suggests this treatment has potential to achieve efficacy against NSCLC bone metastasis in the clinic.

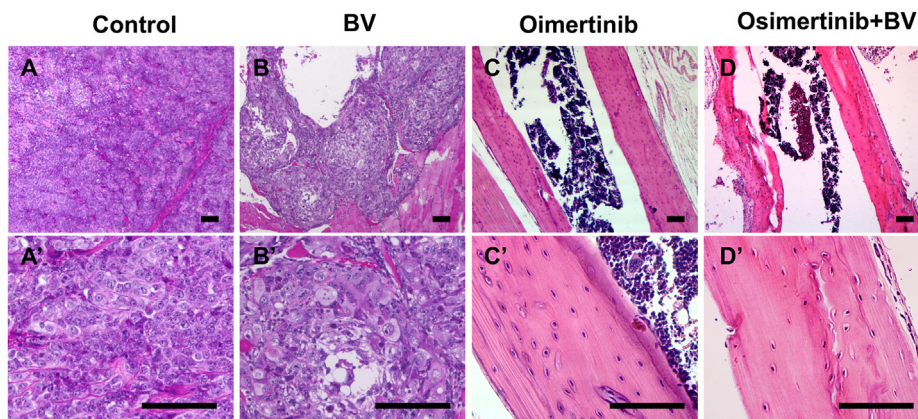
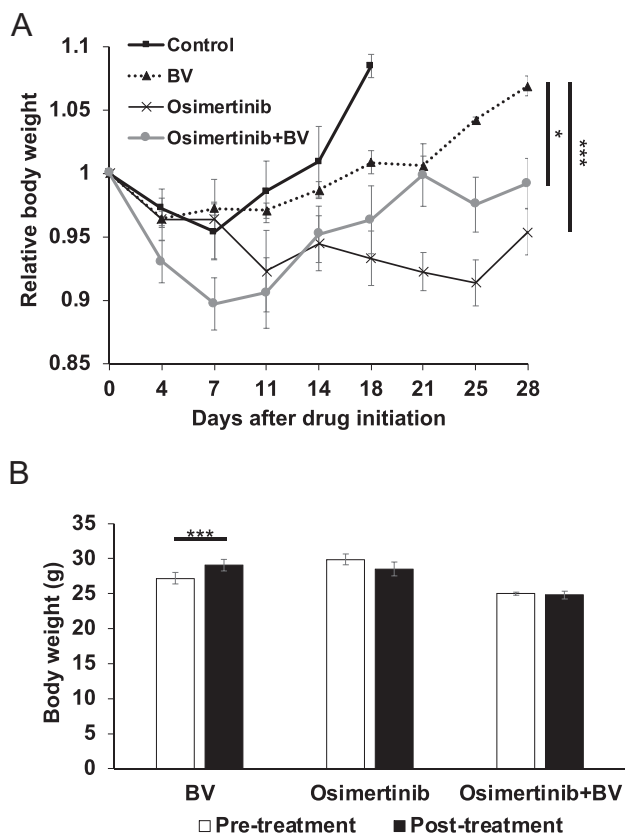


Fig. 5. Tumor histology. (A, A') Control. (B, B') BV alone. (C, C') Oimertinib alone. (D, D') Osimertinib + BV. Scale bars: 100 μm.



**Fig. 6.** Body weight. (A) Line graphs indicate mouse body weight at each time point after the onset of treatment relative to the initial body weight for each treatment and control group. (B) Bar graphs show mouse body weight in each treatment and control group at pre- and post-treatment times. \*  $p < 0.05$ ; \*\*\*  $p < 0.001$ . Error bars:  $\pm$  SEM.

#### Author contributions statement

Conceptualization ideas: TH and RMH; methodology, investigation, validation, formal analysis: TH; investigation, formal analysis and resources: NS, JHP, YS, GZ, NY, KY, KH, HK, SM, and KI; Formal analysis: TH, NS, JHP, YS, GZ, NY, KY, KH, HK, SM, KI, MB, HT, SRS, and RMH; Supervision: RMH; writing and editing: TH, RMH, and SRS.

#### Funding

This research did not receive any specific grant from funding agencies in the public, commercial, or not-for-profit sectors.

#### Declaration of competing interest

The authors declare the following financial interests/personal relationships which may be considered as potential competing interests:

TH, NS, JHP, TH, YS, GZ, KI and RMH are or were unsalaried associates of AntiCancer Inc. AntiCancer Inc. uses PDOX models for contract research. The Authors declare that there are no potential conflicts of interest.

#### References

- [1] Y.J. Cho, Y.M. Cho, S.H. Kim, K.H. Shin, S.T. Jung, H.S. Kim, Clinical analysis of patients with skeletal metastasis of lung cancer, *BMC Cancer* 19 (1) (2019) 303.
- [2] D. Santini, S. Barni, S. Intagliata, A. Falcone, F. Ferrau, D. Galetta, et al., Natural history of non-small-cell lung cancer with bone metastases, *Sci. Rep.* 5 (2015) 18670.
- [3] C. D'Antonio, A. Passaro, B. Gori, E. Del Signore, M.R. Migliorino, S. Ricciardi, et al., Bone and brain metastasis in lung cancer: recent advances in therapeutic strategies, *Ther. Adv. Med. Oncol.* 6 (3) (2014) 101–114.
- [4] H. Tominaga, T. Setoguchi, H. Shimada, S. Nagano, H. Sasaki, Y. Ishidou, et al., Prognostic factors in patients with skeletal-related events at non-small-cell lung cancer diagnosis, *Mol. Clin. Oncol.* 7 (5) (2017) 897–902.
- [5] P. Krawczyk, M. Nicos, R. Ramlau, T. Powrozek, K. Wojas-Krawczyk, S. Sura, et al., The incidence of EGFR-activating mutations in bone metastases of lung adenocarcinoma, *Pathol. Oncol. Res.* 20 (1) (2014) 107–112.
- [6] G.N. Naumov, M.B. Nilsson, T. Cascone, A. Briggs, O. Straume, L.A. Akslen, et al., Combined vascular endothelial growth factor receptor and epidermal growth factor receptor (EGFR) blockade inhibits tumor growth in xenograft models of EGFR inhibitor resistance, *Clin. Cancer Res.* 15 (10) (2009) 3484–3494.
- [7] H. Saito, T. Fukuhara, N. Furuya, K. Watanabe, S. Sugawara, S. Iwasawa, et al., Erlotinib plus bevacizumab versus erlotinib alone in patients with EGFR-positive advanced non-squamous non-small-cell lung cancer (NEJ026): interim analysis of an open-label, randomised, multicentre, phase 3 trial, *Lancet Oncol.* 20 (5) (2019) 625–635.
- [8] J.C. Soria, Y. Ohe, J. Vansteenkiste, T. Reungwetwattana, B. Chewaskulyong, K.H. Lee, et al., Osimertinib in untreated EGFR-mutated advanced non-small-cell lung cancer, *N. Engl. J. Med.* 378 (2) (2018) 113–125.
- [9] H. Akamatsu, S. Teraoka, S. Morita, N. Katakami, M. Tachihara, H. Daga, et al., Phase I/II study of osimertinib with bevacizumab in EGFR-mutated, T790M-positive patients with progressed EGFR-TKIs: West Japan Oncology Group 8715L (WJOG8715L), *Clin. Lung Cancer.* 20 (4) (2019) e492–e494.
- [10] K. Miyake, T. Kiyuna, K. Kawaguchi, T. Higuchi, H. Oshiro, Z. Zhang, et al., Regorafenib regressed a doxorubicin-resistant Ewing's sarcoma in a patient-derived orthotopic xenograft (PDOX) nude mouse model, *Cancer Chemother. Pharmacol.* 83 (5) (2019) 809–815.
- [11] T. Higuchi, K. Miyake, H. Oshiro, N. Sugisawa, N. Yamamoto, K. Hayashi, et al., Trabectedin and irinotecan combination regresses a cisplatin-resistant osteosarcoma in a patient-derived orthotopic xenograft nude-mouse model, *Biochem. Biophys. Res. Commun.* 513 (2) (2019) 326–331.
- [12] T. Brodowicz, K. O'Byrne, C. Manegold, Bone matters in lung cancer, *Ann. Oncol.* 23 (9) (2012) 2215–2222.
- [13] G. Lamberti, E. Andriani, B. Ricciuti, Impact of performance status and age on osimertinib efficacy in patients with EGFR-mutant T790M-positive non-small-cell lung cancer, *J. Thorac. Dis.* 11 (Suppl. 15) (2019) S1831–S1834.
- [14] T. Higuchi, H. Oshiro, Z. Zhang, K. Miyake, N. Sugisawa, Y. Katsuya, et al., Osimertinib regresses an EGFR-mutant cisplatin-resistant lung adenocarcinoma growing in the brain in nude mice, *Transl. Oncol.* 12 (4) (2019) 640–645.
- [15] A.M. Devery, R. Wadekar, S.M. Bokobza, A.M. Weber, Y. Jiang, A.J. Ryan, Vascular endothelial growth factor directly stimulates tumour cell proliferation in non-small cell lung cancer, *Int. J. Oncol.* 47 (3) (2015) 849–856.
- [16] H. Li, K. Takayama, S. Wang, Y. Shiraishi, K. Gotanda, T. Harada, et al., Addition of bevacizumab enhances antitumor activity of erlotinib against non-small cell lung cancer xenografts depending on VEGF expression, *Cancer Chemother. Pharmacol.* 74 (6) (2014) 1297–1305.
- [17] T.E. Stinchcombe, P.A. Janne, X. Wang, E.M. Bertino, J. Weiss, L. Bazhenova, et al., Effect of erlotinib plus bevacizumab vs erlotinib alone on progression-free survival in patients with advanced EGFR-mutant non-small cell lung cancer: a phase 2 randomized clinical trial, *JAMA Oncol.* 17 (3) (2019) 217–223.
- [18] O. Hiranuma, J. Uchino, T. Yamada, Y. Chihara, N. Tamiya, Y. Kaneko, et al., Rationale and design of a phase II trial of osimertinib combined with bevacizumab in patients with untreated epidermal growth factor receptor-mutated non-small-cell lung cancer and malignant pleural and/or pericardial effusion (SPIRAL II study), *Clin. Lung Cancer.* 20 (3) (2019) e402–e406.
- [19] M. Yang, S. Hasegawa, P. Jiang, X. Wang, Y. Tan, T. Chishima, et al., Widespread skeletal metastatic potential of human lung cancer revealed by green fluorescent protein expression, *Cancer Res.* 58 (19) (1998) 4217–4221.